

RESEARCH

Open Access



# Normal lung sparing Tomotherapy technique in stage III lung cancer

Chae-Seon Hong<sup>1</sup>, Sang Gyu Ju<sup>1\*†</sup>, Yong Chan Ahn<sup>1,2\*†</sup>, Gyu Sang Yoo<sup>1</sup>, Jae Myoung Noh<sup>1</sup>, Dongryul Oh<sup>1</sup>, Kwangzoo Chung<sup>1</sup>, Hongryull Pyo<sup>1</sup> and Kwanghyun Jo<sup>1</sup>

## Abstract

**Purpose:** Radiation pneumonitis (RP) has been a challenging obstacle in treating stage III lung cancer patients. Beam angle optimization (BAO) technique for Tomotherapy was developed to reduce the normal lung dose for stage III non-small cell lung cancer (NSCLC). Comparative analyses on plan quality by 3 different Intensity-modulated radiation therapy (IMRT) methods with BAO were done.

**Materials and methods:** Ten consecutive stage IIIB NSCLC patients receiving linac-based static IMRT (L-IMRT) with total 66 Gy in 33 fractions to the PTV were selected. Two additional Tomotherapy-based IMRT plans (helical beam (TH-IMRT) and static beam (TD-IMRT)) were generated on each patient. To reduce the normal lung dose, Beam angles were optimized by using complete and directional block functions in Tomotherapy based on knowledge based statistical analysis. Plan quality was compared with target coverage, normal organ sparing capability, and normal tissue complication probability (NTCP). Actual beam delivery times and risk of RP related with planning target volume (PTV) were also evaluated.

**Results:** The best PTV coverage measured by conformity index and homogeneity index was achievable by TH-IMRT (0.82 and 1.06), followed by TD-IMRT (0.81 and 1.07) and L-IMRT (0.75 and 1.08). Mean lung dose was the lowest in TH-IMRT plan followed by TD-IMRT and L-IMRT, all of which were  $\leq 20$  Gy. TH-IMRT plan could significantly lower the lung volumes receiving low to medium dose levels:  $V_{5-30}$  when compared to L-IMRT plan; and  $V_{5-20}$  when compared to TD-IMRT plan, respectively. TD-IMRT plan was significantly better than L-IMRT with respects to  $V_{20}$  and  $V_{30}$  and there was no significant difference with respect to  $V_{40}$  among three plans. The NTCP of the lung was the lowest in TH-IMRT plan, followed by TD-IMRT and L-IMRT (6.42% vs. 6.53% vs. 8.11%). Beam delivery time was the shortest in TD-IMRT plan followed by L-IMRT. As PTV length increased, NTCP and Mean lung dose proportionally increased significantly in all three plans.

**Conclusion:** Advantageous profiles by TH-IMRT could be achieved by BAO by complete and directional block functions. Current observation could help radiation oncologists to make wise selection of IMRT method for stage IIIB NSCLC.

**Keywords:** Lung cancer, Intensity-modulated radiotherapy, Tomotherapy, Radiation pneumonitis

\* Correspondence: sg.ju@samsung.com; ycahn.ahn@samsung.com; ahnyc@skku.edu

†Equal contributors

<sup>1</sup>Department of Radiation Oncology, Samsung Medical Center, Sungkyunkwan University School of Medicine, Irwon-Ro 81, Gangnam-Gu, Seoul 06351, South Korea

Full list of author information is available at the end of the article



## Introduction

Over one-third of non-small cell lung cancer (NSCLC) patients are diagnosed at stage III. These have usually been the ideal candidates for high dose radiation therapy (RT) with concurrent chemotherapy [1–7]. In order to achieve improved local control and survival, escalation of RT dose should be realized, which, however, is frequently associated with toxicity risk, particularly under concurrent chemotherapy setting. Therefore, it is necessary to limit RT dose to volume of normal organs including the spinal cord, lung, heart and esophagus. Radiation pneumonitis (RP) is the most challenging obstacle and sparing of as much lung volume as possible is very important [8, 9].

The normal lung volume that receives 20 Gy or higher ( $V_{20}$ ) has been used as an important indicator to predict the risk of symptomatic RP [10]. Efforts to limit  $V_{20}$  below 30%, while ensuring conformal dose to the target, however, have often been difficult by conventional three-dimensional conformal RT (3D-CRT) technique. Intensity-modulated RT (IMRT), through the inverse planning technique, can provide better target coverage and more sparing of the surrounding normal organs. IMRT has resulted in better clinical outcomes than 3D-CRT in treating stage III NSCLC patients, by dose escalation with more favorably limited  $V_{20}$  constraint [11–14]. By virtue of the beam delivery method that uses a large number of beamlets, IMRT is well known to increase the lung volume receiving low dose level of 5 Gy ( $V_5$ ), which has also proved to be closely related to the RP risk.  $V_5$  has recently received an high level attention as an important indicator in evaluating the RT plan quality and a few reports recommend to keep  $V_5$  below 60~65% in the patients undergoing RT with concurrent chemotherapy [12, 15]. Though with a few advantages, routine application of IMRT in treating stage III NSCLC patients has been a challenge [16–19]. Tomotherapy, a volumetric modulated arc therapy (VMAT), is a radiation beam delivery system that combines IMRT with a helical beam delivery technique (TomoHelical IMRT [TH-IMRT], Accuray, WI, USA) with a megavoltage CT (MVCT) capability, enabling image-guided radiation therapy [20]. While excellent dosimetric benefits have been noted with TH-IMRT for various disease sites, [21–23] it has not been widely investigated or accepted for the treatment of stage III NSCLC [24, 25].

Different dose profiles are achieved within and around the target, depending on dose constraints and beam delivery methods. Classic IMRT used to put as many equally spaced beams as possible. Plan quality comparisons when using 5, 7 and 9 beams in L-IMRT were done following multi-objective function iteration to determine optimal beam angles by Liu et al., which showed that optimal determination of beam angles was more important

than simple increase of beam numbers to achieve better plan quality [26]. Beam angle optimization (BAO), however, is not an easy task under 360 degrees full arc rotation. For beam angle controlling, complete and directional block functions were developed on the individual basis and incorporated into the treatment planning system (TPS) of Tomotherapy [27, 28]. The incoming beams were to be arranged so that the complete blocks did not allow any beams to pass through them at all, while the directional blocks allowed beams only if they entered PTV first [27, 28].

Linear accelerator has evolved to perform dynamic “volumetric arc” beam delivery with full arc rotation [29, 30]. On the contrary, Tomotherapy has evolved to enable static beam delivery (TomoDirect-IMRT, TD-IMRT) to decrease integral dose [23, 31]. Various types of advanced treatment techniques were employed to reduce normal lung dose, but it is still a major barrier for the RT of stage III NSCLC.

In addition, there are many patient dependent factors that affect the normal lung dose in treatment planning for stage III NSCLC. Understanding of important factors, which are closely related to normal lung dose, is very important to predict complication and select treatment technique for better clinical choice. However, factor analysis related to normal lung dose and treatment technique based on geometrical information of PTV and OARs was not clearly given for RT of stage III NSCLC. We developed a new BAO technique by employing complete and directional block function for Tomotherapy of stage III NSCLC and performed comparative analyses on plan quality with L-IMRT.

## Methods

### Patient selection, simulation, and contouring

Authors selected ten consecutive patients having N3-IIIB NSCLC by virtue of low cervical lymph node involvement, between March 2012 and November 2013. All received definitive high dose L-IMRT (Novalis Tx<sup>®</sup>, Varian, USA) concurrent with weekly chemotherapy (Table 1). All were immobilized by individually customized cradle with foaming material in the supine position before simulation. Four-dimensional CT (4D-CT) was obtained using respiration management system (RPM<sup>®</sup>; Varian, USA), which was segmented into 10 respiratory phases, and all image sets were transferred into TPS (Pinnacle3<sup>®</sup>, version 9.2; Philips Medical System, USA). With reference to all available clinical information, the gross tumor volume (GTV) on each respiratory phase was delineated to generate the internal target volume (ITV). The clinical target volume (CTV) was generated by expansion of ITV with 5 mm margins in all directions, which was modified so that the expanded ITV did not exceed the actual anatomic boundaries such as the bone

**Table 1** Patients' characteristics

	Gender	Age	Primary tumor	Low neck involvement	Clinical stage	Histology
1	Female	72 years	LUL	Ipsilateral	T1 N3	Adenocarcinoma
2	Female	52 years	RLL	Ipsilateral	T1 N3	Adenocarcinoma
3	Male	58 years	RLL	Ipsilateral	T2 N3	Squamous
4	Male	49 years	RUL/RLL	Ipsilateral	T4 N3	Adenocarcinoma
5	Male	65 years	RUL	Ipsilateral	T3 N3	Adenocarcinoma
6	Male	44 years	LLL	Ipsilateral	T1 N3	Adenocarcinoma
7	Male	67 years	LLL	Contralateral	T2 N3	Squamous
8	Male	58 years	LLL	Contralateral	T2 N3	Squamous
9	Male	64 years	RUL	Bilateral	T2 N3	Adenocarcinoma
10	Male	49 years	RLL	Bilateral	T2 N3	Adenocarcinoma

RUL right upper lobe, RLL right lower lobe, LUL left upper lobe, LLL left lower lobe

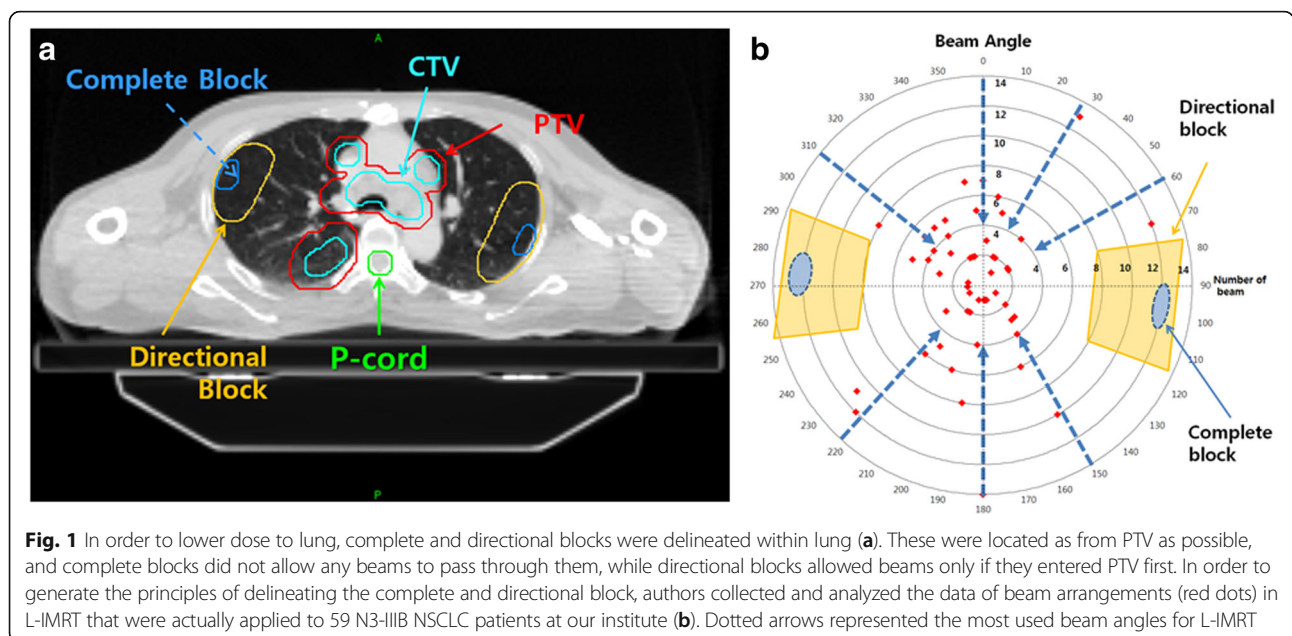
(spine, rib), tracheobronchial cartilage, chest wall, and great vessels. The planning target volume (PTV) was generated by expansion of CTV with 5 mm margin (Fig. 1). The organs at risk (OARs) were delineated including the spinal cord, normal lungs (both lung – PTV), heart and esophagus. The planning volume for the spinal cord (P-cord) was generated by adding 5 mm margin to the actual spinal cord, which was optionally reduced to 3 mm if the PTV was very close to the spinal cord.

**Generation of IMRT plans and beam angle optimization**

For dosimetric comparison, three different IMRT plans on each patient were generated. All patients were actually treated by linear accelerator-based single isocenter step and shoot L-IMRT concurrent with weekly chemotherapy using Novalis Tx<sup>®</sup>,(Varian, USA). The numbers of static beams in L-IMRT plans were six in eight

patients, five in one, and seven in one, and the same beam angles were used in TD-IMRT plans. Beam angles were optimized on trial and error basis based on BAO by Liu et al. [26].

Two additional Tomotherapy<sup>®</sup>-based IMRT plans, TH-IMRT and TD-IMRT, were generated on each patient. In order to help determine optimized beam angles through complete and directional blocks functions, pseudo-OARs (complete and directional block) within the lung were delineated so that they were located as far from PTV as possible (Fig. 1a). Because the shape, size and geometric relations between the CTV and OARs were not the same among patients, application of the pseudo-OARs in the same way was not possible. In order to generate the principles of delineating the pseudo-OARs based on knowledge based statistical analysis, authors collected and analyzed the data of beam arrangements



in L-IMRT that were actually applied to 59 N3-IIIB NSCLC patients at our institute (red dots in Fig. 1b). The ideal beam directions (dotted arrows in Fig. 1b) that coincided with the method proposed by Liu et al. [26]. Pseudo-OARs should not be hit by any incoming beams and should be  $\geq 1.5$  cm from the closest PTV margin. Principally pseudo-OARs are to be delineated on both sides, but could be omitted on one side where the distance from the closest PTV was less than 1.5 cm. Circular directional block of 5 cm radius and complete block of 1.5 cm radius were to be located as far from the PTV as possible along the superior-inferior dimension of the PTV. The size and shape of the pseudo-OARs were modified considering the PTV location and the optimized dose profiles.

The angles of incoming beams in all three plans were optimized and determined according to the same rules policy. In both TH-IMRT and TD-IMRT plans, field width of 2.5 cm, modulation factor of 2.0, and pitch of 0.287 were used to avoid the thread effect [32]. In all three plans, 6-MV photon beams were used and dose calculation was done using the collapsed-cone convolution algorithm [33, 34].

**Dose constraints and optimization**

All three plans followed the internal guideline on the dose constraints, which were stricter than RTOG protocol 0617 (Table 2) [35]. Two constraints were set at the highest priority level: 95% of PTV volume should receive at least 100% of the prescription dose (66 Gy/33 fractions;  $D_{95} \geq 66$  Gy); and the maximum dose to P-cord should not exceed 45 Gy ( $D_{max} < 45$  Gy). In order to achieve as homogenous dose distribution as possible

within and around the PTV, 99% of the PTV volume should receive at least 93% of the prescription dose ( $D_{99} \geq 61.38$  Gy) and the volume receiving  $\geq 110\%$  of the prescribed dose (72.6 Gy) should not be greater than 1 cm<sup>3</sup> in total volume if within the PTV and/or in contiguous volume if outside the PTV ( $V_{72.6 \text{ Gy}} \leq 1 \text{ cm}^3$ ).

The constraints at the second priority level were to limit the radiation dose to the lungs: the average lung dose ( $D_{mean}$ ) should not exceed 20 Gy; and the lung volume receiving 5 Gy ( $V_5$ ), 10 Gy ( $V_{10}$ ) and 20 Gy ( $V_{20}$ ) should not exceed 65, 45 and 35% of normal lung volume, respectively. The same dose constraints were applied to the pseudo-OARs.

The constraints at the third and fourth priority levels were to limit the dose to the heart and esophagus, respectively. The constraints at the third level were to limit the radiation dose to the heart: the heart volume receiving 40 Gy ( $V_{40}$ ), 45 Gy ( $V_{45}$ ) and 60 Gy ( $V_{60}$ ) should not exceed 100, 66 and 33% of the heart volume, respectively. The lowest level constraint was to limit the dose to the esophagus:  $D_{mean}$  to the esophagus should not exceed 34 Gy.

For each plan, the same number of iteration was used during dose optimization process. During inverse planning, once PTV constraints were reached, the optimization was continued to reduce the doses to OARs until the iteration limit while maintaining PTV dose. For dose comparison, all plans were normalized to cover 95% of the PTV with the prescription dose (66 Gy).

**Evaluation of IMRT plans**

All data including calculated dose and contour information of three IMRT plans on each patient were transferred to MIM Maestro® (MIM Software Inc., USA) using the DICOMRT protocol, and objective comparisons of the dose and volume parameters were performed. To evaluate the PTV dose coverage, Conformity index (CI) and Homogeneity index (HI) were used. CI is the ratio of the prescription volume to the PTV, [36] and was calculated as the equation below:

$$CI = \frac{PTV_{PIV}^2}{PTV \times PIV} \tag{1}$$

The  $PTV_{PIV}$  is the PTV encompassed within the volume covered by the prescription isodose surface (PIV). CI value of 1 means a perfect conformation, where the prescription isodose is identical to the target volume, and better conformity is achieved as CI value approaches 1.

HI is an indication of the dose uniformity within the PTV, defined as a ratio the dose delivered to 5% and 95% of the PTV volumes, respectively [37]. HI value of 1

**Table 2** Dose constraints for inverse planning

Priority	Structure	Constraints
1	PTV	$D_{95} \geq 66$ Gy (100%) $D_{99} \geq 61.38$ Gy (93%) $V_{72.6 (110\%)} \leq 1 \text{ cm}^3$
1	P-cord <sup>a</sup>	$D_{max} \leq 45$ Gy
2	Normal lung (both lung - PTV)	$D_{mean} \leq 20$ Gy $V_5 \leq 65\%$ $V_{10} \leq 45\%$ $V_{20} \leq 35\%$
3	Heart	$V_{40} < 100\%$ $V_{45} < 66\%$ $V_{60} < 33\%$
4	Esophagus	$D_{mean} \leq 34$ Gy

$D_V$  D dose delivered to V% of organ volume,  $V_D$  absolute or percentage of organ volume receiving D Gy or higher,  $D_{max}$  maximum dose,  $D_{mean}$  mean dose, OARs organ at risks

<sup>a</sup>P-cord means the planning volume for the spinal cord which was generated by adding 3-5 mm margin to the actual spinal cord

is the ideal value that indicates a uniform dose distribution within the PTV.

$$HI = \frac{D_5}{D_{95}} \tag{2}$$

For comparative evaluation of radiobiological effects on normal organs including the lung, spinal cord, heart and esophagus, the normal tissue complication probability (NTCP) using the Kutcher-Burman histogram reduction scheme in conjunction with the Lyman model [38–43] was used by applying the same calculation parameters that used by Song [43]. The comparison of NTCP's was possible because the dose calculation algorithms were the same between the TPS (collapsed-cone convolution algorithm) [44, 45]. In addition, several relevant dosimetric parameters on these organs were used for comparisons:  $V_5, V_{10}, V_{15}, V_{20}, V_{30}, V_{40}$  and  $D_{mean}$  of the lungs;  $D_{max}$  to P-cord;  $V_{45}$  and  $V_{60}$  of the heart; and  $V_{50}$  and  $V_{60}$  of the esophagus, respectively.

The actual beam delivery times by each plan, defined as the time from the first beam-on till the last beam-off, were measured to compare the machine workloads, which, in turn, could be used in patient throughput estimation, assuming that the times needed for patient setup before the first beam-on were equivalent to each other.

In order to evaluate the impacts of PTV-related factors on the risk of lung toxicity, the superior to inferior length of PTV (PTV length) and PTV overlapping with the normal lung ( $PTV \cap Lung$ ), in addition to PTV itself, were calculated.

The Wilcoxon signed-rank test and the Bonferroni correction (SAS version 9.4, SAS Institute, Cary, NC, USA) were used to compare the dosimetric parameters and the beam delivery time between plans one by one. The Spearman correlation test was used to determine the association between PTV-related factors and the dosimetric parameters and NTCP of the lung. Two-tailed  $p$  value <0.05 was considered statistically significant.

## Results

### Treatment plan evaluation

The comparisons of dosimetric parameters and beam delivery times by 3 IMRT methods are summarized in Table 3. The best PTV coverage measured by CI and HI was achievable by TH-IMRT (0.82 and 1.06), followed by TD-IMRT (0.81 and 1.07) and L-IMRT (0.75 and 1.08). In one by one comparison, both TH-IMRT and TD-IMRT exhibited significantly better CI and HI than L-IMRT (all  $p$  values were 0.006) (Fig. 2).

The NTCP and  $D_{max}$  of the spinal cord were the lowest in TH-IMRT plan followed by TD-IMRT and L-

**Table 3** Comparisons of dosimetric parameters and beam delivery time

Parameters		L-IMRT	TH-IMRT	TD-IMRT	$p^a$		
		Median (IQR)	Median (IQR)	Median (IQR)	L-IMRT vs. TH-IMRT	L-IMRT vs. TD-IMRT	TH-IMRT vs TD-IMRT
PTV	CI	0.75 (0.72, 0.81)	0.82 (0.79, 0.85)	0.81 (0.77, 0.83)	0.006	0.006	0.580
	HI	1.08 (1.07, 1.08)	1.06 (1.05, 1.06)	1.07 (1.05, 1.07)	0.006	0.006	0.317
P-cord	NTCP	0.82% (0.71, 0.92)	0.34% (0.23, 0.48)	0.43% (0.28, 0.55)	0.006	0.006	0.393
	$D_{max}$	46.44 Gy (45.56, 47.21)	44.93 Gy (40.35, 45.33)	45.55 Gy (41.41, 46.68)	0.029	0.317	0.194
Normal Lung	NTCP	8.11% (4.90, 10.11)	6.42% (3.67, 7.47)	6.53% (4.95, 9.51)	0.006	1.000	0.082
	$D_{mean}$	17.83 Gy (14.98, 19.16)	16.49 Gy (13.49, 17.30)	16.60 Gy (14.98, 18.78)	0.006	1.000	0.082
	$V_5$	62.46% (54.08, 71.35)	61.46% (50.92, 68.01)	65.83% (58.94, 72.58)	0.006	0.393	0.006
	$V_{10}$	48.48% (43.71, 53.45)	43.76% (35.66, 49.68)	51.87% (45.52, 56.77)	0.006	0.967	0.006
	$V_{15}$	40.63% (37.17, 45.77)	34.56% (28.11, 39.09)	38.81% (34.66, 45.60)	0.006	0.580	0.001
	$V_{20}$	35.47% (30.92, 37.54)	28.02% (23.35, 31.08)	30.30% (27.79, 34.55)	0.006	0.006	0.006
	$V_{30}$	23.99% (20.37, 26.77)	19.65% (16.30, 21.70)	19.75% (17.69, 21.23)	0.006	0.029	0.580
	$V_{40}$	13.26% (12.07, 18.24)	13.61% (11.35, 15.94)	12.63% (11.78, 14.91)	1.000	1.000	1.000
Heart	NTCP	27.70% (23.75, 33.50)	27.24% (23.90, 33.10)	27.44% (24.07, 32.40)	1.000	1.000	1.000
	$V_{45}$	6.71% (0.95, 21.71)	4.10% (0.20, 11.15)	4.66% (0.90, 10.06)	0.023	0.023	1.000
	$V_{60}$	1.92% (0.04, 7.02)	1.65% (0.00, 4.25)	1.41% (0.05, 4.53)	0.117	0.047	1.000
Esophagus	NTCP	35.57% (21.88, 46.54)	33.05% (17.92, 42.89)	36.91% (22.89, 45.17)	0.252	1.000	0.082
	$V_{50}$	41.79% (24.36, 48.55)	38.43% (18.63, 48.17)	42.77% (22.23, 49.65)	0.059	0.580	0.393
	$V_{60}$	29.55% (10.26, 38.90)	25.28% (9.35, 39.00)	30.25% (11.75, 39.26)	0.146	1.000	0.018
Beam delivery time		8.4 min (6.98, 10.18)	10.1 min (9.05, 11.90)	7.3 min (6.23, 8.90)	0.252	0.375	0.006

CI conformity index, HI homogeneity index,  $V_D$  the percentage of organ volume receiving D Gy or higher,  $D_{mean}$  mean dose,  $D_{max}$  maximum dose, NTCP normal tissue complication probability, IQR interquartile range (Q1, Q3)

<sup>a</sup>The Wilcoxon signed rank test was used by the Bonferroni correction for multiple testing



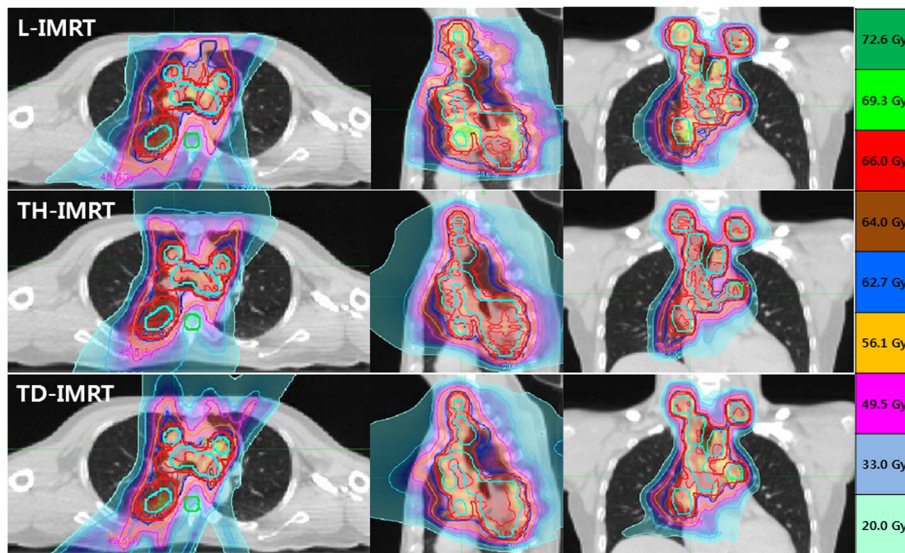


**Fig. 2** Isodose distribution of an example case in axial, sagittal, and coronal sections by L-IMRT, TH-IMRT and TD-IMRT. Apparent dose distribution looked better conformed to PTV in order of TH-IMRT, TD-IMRT and L-IMRT

IMRT (0.34% and 44.93 Gy vs. 0.43% and 45.55 Gy vs. 0.82% and 46.44 Gy). In one by one comparison, the NTCP's of TH-IMRT and TD-IMRT plans were significantly lower than L-IMRT ( $p = 0.006$ ) and  $D_{max}$  of TH-IMRT was significantly lower than L-IMRT ( $p = 0.029$ ). The NTCP of the lung was the lowest in TH-IMRT plan, followed by TD-IMRT and L-IMRT (6.42% vs. 6.53% vs. 8.11%). In one by one comparison, the difference between TH-IMRT and L-IMRT plans was significant ( $p = 0.006$ ). Based on the dose-volume histogram comparison, the lung volume receiving low to medium dose

level was the smallest in TH-IMRT plan (Fig. 3).  $D_{mean}$  was the lowest in TH-IMRT plan followed by TD-IMRT and L-IMRT (16.49 Gy vs. 16.60 Gy vs. 17.83 Gy), all of which were  $\leq 20$  Gy and satisfied the predefined constraint, and the difference between TH-IMRT and L-IMRT plans was significant ( $p = 0.006$ ). TH-IMRT plan was able to satisfy other three constraints on the lung ( $V_5 \leq 65\%$ ,  $V_{10} \leq 45\%$  and  $V_{20} \leq 35\%$ ) and L-IMRT plan satisfied  $V_5$  constraint only. TH-IMRT plan could significantly lower the lung volumes receiving low to medium dose levels:  $V_{5-30}$  when compared to L-IMRT plan; and

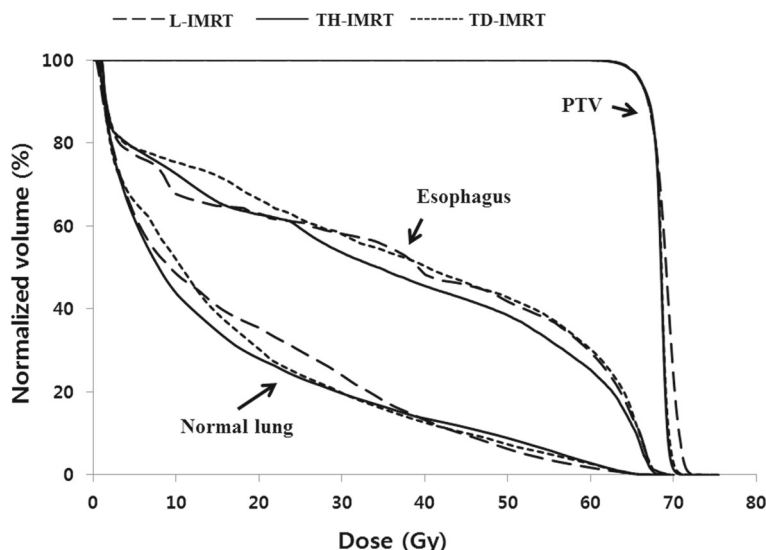


**Fig. 3** Median dose-volume histograms of all ten patients for PTV, esophagus, and normal lung by L-IMRT, TH-IMRT and TD-IMRT

$V_{5-20}$  when compared to TD-IMRT plan, respectively. TD-IMRT plan was significantly better than L-IMRT with respects to  $V_{20}$  and  $V_{30}$  and there was no significant difference with respect to  $V_{40}$  among three plans.

The NTCP of the heart was the lowest in TH-IMRT plan followed by TD-IMRT and L-IMRT (27.24% vs. 27.44% vs. 27.70%).  $V_{45}$  was the lowest in TH-IMRT plan followed by TD-IMRT and L-IMRT (4.10% vs. 4.66% vs. 6.71%) and  $V_{60}$  was the lowest in TD-IMRT plan followed by TH-IMRT and L-IMRT (1.41% vs. 1.65% vs. 1.92%), respectively.  $V_{45}$  of TH-IMRT and TD-IMRT plans were significantly lower than L-IMRT ( $p = 0.023$ ) and  $V_{60}$  of TD-IMRT was significantly lower than L-IMRT ( $p = 0.047$ ).

The NTCP of the esophagus was the lowest in TH-IMRT plan followed by L-IMRT and TD-IMRT (33.05% vs. 35.57% vs. 36.91%), however, there was no significant differences.  $V_{50}$  and  $V_{60}$  were the lowest in TH-IMRT plan followed by L-IMRT and TD-IMRT (38.43% and 25.28% vs. 41.79% and 29.55% vs. 42.77% and 30.25%).  $V_{60}$  of TH-IMRT was significantly lower than TD-IMRT ( $p = 0.018$ ).

The beam delivery time was the shortest in TD-IMRT plan followed by L-IMRT and TH-IMRT (7.3 min vs. 8.4 min vs. 10.1 min), and that of TD-IMRT plan was significantly shorter than TH-IMRT ( $p = 0.006$ ).

**Correlation between PTV-related parameters on lung toxicity risk**

The median values of PTV, superior-inferior PTV length, and PTV volume overlapping with lung (PTV  $\cap$  Lung) of all patients were 479 cm<sup>3</sup> (interquartile range [IQR]: 417~606 cm<sup>3</sup>), 18.0 cm (IQR: 15.2~19.8 cm) and 5.3% (IQR: 3.5%~5.9%), respectively. The estimated impacts of PTV and PTV-related factors on the risk of RP in three different plans are summarized in Table 4. In all three plans, there was no significant correlation between RP risk and PTV itself or PTV  $\cap$  Lung. However, as PTV length increased, NTCP and  $D_{mean}$  proportionally increased in all three plans significantly, which was the most prominent in TH-IMRT plan ( $p = 0.005$ ). Along with increasing PTV length,  $V_{5-20}$  in L-IMRT,  $V_{5-40}$  in TH-IMRT, and  $V_{15-20}$  in TD-IMRT plans increased significantly as well (all  $p$  values <0.05).

**Discussion**

There are a few challenging issues of the target delineation and the interplay effects caused by respiratory and multi-leaf motions, particularly in treating lung cancer patients [17–19, 46]. Delineation of the ITV, which reflects the target motion by respiratory cycle, has been routinely performed following 4D-CT, and several previous studies have endorsed that the interplay effects could become averaged out (smearing) to the negligible level during the multi-fractioned RT course [47, 48].

**Table 4** Comparison of correlation coefficient between parameters related with planning target volume (PTV) and lung

Parameters	Lung	L-IMRT	$\rho^c$	TH-IMRT	$\rho^c$	TD-IMRT	$\rho^c$	
PTV	NTCP	-0.309	0.385	-0.261	0.467	-0.442	0.200	
	$D_{mean}$	-0.309	0.385	-0.261	0.467	-0.442	0.200	
	$V_5$	-0.273	0.446	-0.321	0.366	-0.406	0.244	
	$V_{10}$	-0.236	0.511	-0.224	0.533	-0.345	0.328	
	$V_{15}$	-0.273	0.446	-0.358	0.310	-0.539	0.108	
	$V_{20}$	-0.272	0.446	-0.321	0.366	-0.406	0.244	
	$V_{30}$	-0.236	0.511	-0.224	0.533	-0.345	0.328	
	$V_{40}$	-0.297	0.405	-0.152	0.676	-0.4303	0.215	
	PTV length <sup>a</sup>	NTCP	0.663	0.037	0.802	0.005	0.632	0.049
		$D_{mean}$	0.663	0.039	0.802	0.005	0.632	0.049
$V_5$		0.657	0.039	0.687	0.028	0.523	0.121	
$V_{10}$		0.839	0.002	0.729	0.017	0.498	0.143	
$V_{15}$		0.851	0.002	0.802	0.005	0.644	0.044	
$V_{20}$		0.821	0.004	0.815	0.004	0.729	0.017	
$V_{30}$		0.547	0.102	0.711	0.021	0.553	0.097	
$V_{40}$		0.322	0.364	0.778	0.008	0.505	0.137	
PTV $\cap$ Lung <sup>b</sup>		NTCP	0.067	0.855	0.103	0.777	-0.079	0.829
		$D_{mean}$	0.067	0.855	0.103	0.777	-0.079	0.829
	$V_5$	0.103	0.777	0.152	0.676	0.115	0.751	
	$V_{10}$	0.055	0.881	-0.018	0.960	-0.139	0.701	
	$V_{15}$	0.03	0.934	-0.018	0.960	-0.127	0.726	
	$V_{20}$	-0.055	0.881	-0.042	0.907	-0.103	0.777	
	$V_{30}$	-0.018	0.960	0.115	0.751	-0.152	0.676	
	$V_{40}$	-0.03	0.934	0.273	0.446	0.018	0.960	

PTV planning target volume, NTCP normal tissue complication probability,  $V_D$  the percentage of organ volume receiving D Gy or higher,  $D_{mean}$  mean dose  
<sup>a</sup>PTV length means the superior-inferior length of the PTV  
<sup>b</sup>PTV  $\cap$  Lung means the PTV volume overlapping with the normal lung  
<sup>c</sup>All  $p$  values were calculated by the Spearman correlation test

Beam delivery by full arc rotation, in general, has the merit of high conformity within the deep tissues, and, at the same time, has the demerit of increased integral dose to the peripheral body parts. Because the relative electron density of the lung is around 0.3, the range of radiation in the normal lung that surrounds solid tumor becomes naturally longer than in other body parts. In high dose RT settings, coupled with low relative electron density, the lung volume receiving low to moderate dose level frequently becomes quite large in proportion to volume and superior to inferior length of target. A few reports currently recommend to keep  $V_5$  below 60~65% in high dose RT and concurrent chemotherapy setting [12, 15]. In this context, beam delivery from within restricted ranges, rather than full arc rotation, is essentially necessary to reduce the lung volume receiving low to moderate dose [26].

BAO can be realized in different ways by inverse planning algorithm (IPA) of the TPS and beam delivery technique. In this context, direct comparison of BAO techniques with Linear accelerator based volumetric modulated arc therapy (L-VMAT) and TH-IMRT is not an easy task because they have different IPS and beam delivery options. A few reports introduced L-VMAT techniques for treatment of stage III NSCLC, not included in this study [49, 50]. General consensus of these was full arc VMAT can increase lung volume receiving low to moderate dose in RT for stage III NSCLC. They recommended the use of partial arc VMAT or hybrid (partial arc combine with static IMRT beams) technique, which is another type of BAO for L-VMAT, to meet criteria for normal lung dose instead of full arc VMAT. Through indirect comparison with these report, our data showed reasonable and comparable result in normal lung sparing capability.

TH-IMRT is capable to generate superior dosimetric profiles to L-IMRT by full arc helical beam delivery method, and has demonstrated favorable clinical outcomes in various disease sites [20–23]. Though there have been many clinical studies implementing IMRT in treating lung cancer, clinical use of TH-IMRT has been rather less active, mainly in fear of increased integral dose, most of which can be delivered to the normal lung [25, 51]. With the same general consensus compared to full arc VMAT, two studies using TH-IMRT without BAO reported that an increased  $V_{5-10}$  was associated with serious lung toxicity [24, 43]. Determination of optimal beam angles that can reduce the normal lung volume receiving clinically significant radiation dose is not an easy task in TH-IMRT, which deliver radiation dose through Helical beam delivery technique, rapid rotating of the gantry with table translation. Liu et al., through multi-objective optimization, proposed the beam angles confined within rather narrow ranges of anterior and posterior oblique directions, which generated the typical “butterfly-like” shape [26]. This directional blocking concept could reduce the low dose lung volume considerably, when compared to the previous reports [24, 43]. In this respect, our study is unique in that, for the first time, authors further controlled the beam angles passing through the normal lung, which was far from the target, by using the complete blocking in addition to the directional blocking function (Fig. 1) in RT for stage III NSCLC. Since the complete blocks can limit the freedom of beam angle more, and, as a result, can compromise the target coverage, it is advised to delineate this as small as possible and as far from the target as possible. Meanwhile, application of rather generous and large directional blocks outside the target may be allowed.

Though a new beam delivery method, as in TD-IMRT, has been introduced to Tomotherapy-based static IMRT,

the dosimetric characteristics have not been fully addressed as of yet for treating stage III NSCLC. Furthermore, the significance of BAO policy by complete and directional block functions, which is relatively new and advanced, has not been properly evaluated, and the current study is the first comprehensive and comparative evaluation of 3 different IMRT techniques for treating stage III NSCLC.

## Conclusions

Through the dosimetric comparisons among 3 IMRT plans, a few remarkable findings could be summarized. First, CI and HI could have been significantly improved by TH- and TD-IMRT when compared to L-IMRT. Second, TD-IMRT seems to be more advantageous over L-IMRT on  $V_{20}$  and  $V_{30}$ , but more disadvantageous over TH-IMRT on  $V_{5-20}$ . Third, TH-IMRT only could have fulfilled all dosimetric constraints of the lung, which is contradictory to the previous belief that helical beam delivery can increase the integral dose. Authors would strongly believe that these advantageous profiles by TH-IMRT could be achieved by BAO policy employed in the current study. Fourth, beam delivery time is significantly longer by TH-IMRT than TD-IMRT. Authors would wish that the current observation together with dosimetric comparison could serve to help radiation oncologists in making wise selection of IMRT technique.

## Abbreviations

4D-CT: Four-dimensional CT; BAO: Beam angle optimization; CI: Conformity index; CTV: Clinical target volume;  $D_{max}$ : Maximum dose;  $D_{mean}$ : Mean dose;  $D_v$ : D dose delivered to V% of organ volume; GTV: Gross tumor volume; HI: Homogeneity index; IMRT: Intensity-modulated radiation therapy; IPA: Inverse planning algorithm; IQR: Interquartile range (Q1, Q3); ITV: Internal target volume; L-IMRT: Linac-based static IMRT; LLL: Left lower lobe; LUL: Left upper lobe; L-VMAT: Linear accelerator based volumetric modulated arc therapy; MVCT: Megavoltage computed tomography; NSCLC: Non-small cell lung cancer; NTCP: Normal tissue complication probability; OAR: Organs at risk; P-cord: Planning volume for the spinal cord; PTV: Planning target volume; RLL: Right lower lobe; RP: Radiation pneumonitis; RT: Radiation therapy; RUL: Right upper lobe; TD-IMRT: TomoDirect-IMRT; TH-IMRT: TomoHelical-IMRT; TPS: Treatment planning system;  $V_D$ : Percentage of organ volume receiving D Gy or higher; VMAT: Volumetric modulated arc therapy

## Acknowledgements

Not applicable.

## Funding

This work was supported by the research program, NRF-2015R1C1A1A02036613 (Korea).

## Availability of data and materials

The datasets analyzed during the current study are available from the corresponding author on reasonable request.

## Authors' contributions

Conception, design, and drafting the manuscript were performed by SGJ, YCA, and C-SH. Data collection and interpreting were performed by GSY, JMN, DO, KC, HP, and KJ. All authors read and approved the final manuscript.

## Ethics approval and consent to participate

Not applicable.



**Consent for publication**

Not applicable.

**Competing interests**

The authors declare that they have no competing interests.

**Publisher's Note**

Springer Nature remains neutral with regard to jurisdictional claims in published maps and institutional affiliations.

**Author details**

<sup>1</sup>Department of Radiation Oncology, Samsung Medical Center, Sungkyunkwan University School of Medicine, Irwon-Ro 81, Gangnam-Gu, Seoul 06351, South Korea. <sup>2</sup>Department of Medical Device Management and Research, SAHST, Sungkyunkwan University, Irwon-Ro 81, Gangnam-Gu, Seoul 06351, South Korea.

Received: 17 July 2017 Accepted: 14 October 2017

Published online: 06 November 2017

**References**

- The World Health Report; 2003. The World Health Organization (WHO). [http://www.who.int/whr/2003/en/whr03\\_en.pdf](http://www.who.int/whr/2003/en/whr03_en.pdf).
- Bentzen SM, Trotti A. Evaluation of early and late toxicities in chemoradiation trials. *J Clin Oncol*. 2007;25:4096–103.
- Jett JR, Schild SE, Keith RL, Kesler KA, American College of Chest P. Treatment of non-small cell lung cancer, stage IIIb: ACCP evidence-based clinical practice guidelines (2nd edition). *Chest*. 2007;132:2665–76S.
- Scott WJ, Howington J, Feigenberg S, Movsas B, Pisters K, American College of Chest P. Treatment of non-small cell lung cancer stage I and stage II: ACCP evidence-based clinical practice guidelines (2nd edition). *Chest*. 2007;132:234S–42S.
- van Baardwijk A, Wanders S, Boersma L, Borger J, Ollers M, Dingemans AM, et al. Mature results of an individualized radiation dose prescription study based on normal tissue constraints in stages I to III non-small-cell lung cancer. *J Clin Oncol*. 2010;28:1380–6.
- Wang L, Correa CR, Zhao L, Hayman J, Kalemkerian GP, Lyons S, et al. The effect of radiation dose and chemotherapy on overall survival in 237 patients with stage III non-small-cell lung cancer. *Int J Radiat Oncol Biol Phys*. 2009;73:1383–90.
- Kang KM, Jeong BK, Ha IB, Chai GY, Lee GW, Kim HG, et al. Concurrent chemoradiotherapy for elderly patients with stage III non-small cell lung cancer. *Radiat Oncol J*. 2012;30:140–5.
- Bastos BR, Hatoum GF, Walker GR, Tolba K, Takita C, Gomez J, et al. Efficacy and toxicity of chemoradiotherapy with carboplatin and irinotecan followed by consolidation docetaxel for unresectable stage III non-small cell lung cancer. *J Thorac Oncol*. 2010;5:533–9.
- Vogelius IS, Westerly DC, Cannon GM, Mackie TR, Mehta MP, Sugie C, et al. Intensity-modulated radiotherapy might increase pneumonitis risk relative to three-dimensional conformal radiotherapy in patients receiving combined chemotherapy and radiotherapy: a modeling study of dose dumping. *Int J Radiat Oncol Biol Phys*. 2011;80:893–9.
- Graham MV, Purdy JA, Emami B, Harms W, Bosch W, Lockett MA, et al. Clinical dose-volume histogram analysis for pneumonitis after 3D treatment for non-small cell lung cancer (NSCLC). *Int J Radiat Oncol Biol Phys*. 1999;45:323–9.
- Christian JA, Bedford JL, Webb S, Brada M. Comparison of inverse-planned three-dimensional conformal radiotherapy and intensity-modulated radiotherapy for non-small-cell lung cancer. *Int J Radiat Oncol Biol Phys*. 2007;67:735–41.
- Liu HH, Wang X, Dong L, Wu Q, Liao Z, Stevens CW, et al. Feasibility of sparing lung and other thoracic structures with intensity-modulated radiotherapy for non-small-cell lung cancer. *Int J Radiat Oncol Biol Phys*. 2004;58:1268–79.
- Jiang ZQ, Yang K, Komaki R, Wei X, Tucker SL, Zhuang Y, et al. Long-term clinical outcome of intensity-modulated radiotherapy for inoperable non-small cell lung cancer: the MD Anderson experience. *Int J Radiat Oncol Biol Phys*. 2012;83:332–9.
- Noh JM, Kim JM, Ahn YC, Pyo H, Kim B, Oh D, et al. Effect of radiation therapy techniques on outcome in N3-positive IIIB non-small cell lung cancer treated with concurrent Chemoradiotherapy. *Cancer Res Treat*. 2016;48:106–14.
- Yom SS, Liao Z, Liu HH, Tucker SL, CS H, Wei X, et al. Initial evaluation of treatment-related pneumonitis in advanced-stage non-small-cell lung cancer patients treated with concurrent chemotherapy and intensity-modulated radiotherapy. *Int J Radiat Oncol Biol Phys*. 2007;68:94–102.
- Lievens Y, Nulens A, Gaber MA, Defraene G, De Wever W, Stroobants S, et al. Intensity-modulated radiotherapy for locally advanced non-small-cell lung cancer: a dose-escalation planning study. *Int J Radiat Oncol Biol Phys*. 2011;80:306–13.
- Warren M, Webster G, Ryder D, Rowbottom C, Favier-Finn C. An isotoxic planning comparison study for stage II-III non-small cell lung cancer: is intensity-modulated radiotherapy the answer? *Clin Oncol (R Coll Radiol)*. 2014;26:461–7.
- Guckenberger M, Kavanagh A, Partridge M. Combining advanced radiotherapy technologies to maximize safety and tumor control probability in stage III non-small cell lung cancer. *Strahlenther Onkol*. 2012;188:894–900.
- Murshed H, Liu HH, Liao Z, Barker JL, Wang X, Tucker SL, et al. Dose and volume reduction for normal lung using intensity-modulated radiotherapy for advanced-stage non-small-cell lung cancer. *Int J Radiat Oncol Biol Phys*. 2004;58:1258–67.
- Mackie TR, Holmes T, Swerdloff S, Reckwerdt P, Deasy JO, Yang J, et al. Tomotherapy: a new concept for the delivery of dynamic conformal radiotherapy. *Med Phys*. 1993;20:1709–19.
- Murthy V, Krishnatry R, Mallik S, Master Z, Mahantshetty U, Shrivastava S. Helical tomotherapy-based hypofractionated radiotherapy for prostate cancer: a report on the procedure, dosimetry and preliminary clinical outcome. *J Cancer Res Ther*. 2013;9:253–60.
- Hauswald H, Habl G, Krug D, Kehle D, Combs SE, Bermejo JL, et al. Whole brain helical Tomotherapy with integrated boost for brain metastases in patients with malignant melanoma—a randomized trial. *Radiat Oncol*. 2013;8:234.
- Franco P, Catuzzo P, Cante D, La Porta MR, Sciacero P, Girelli G, et al. TomoDirect: an efficient means to deliver radiation at static angles with tomotherapy. *Tumori*. 2011;97:498–502.
- Meng LL, Feng LC, Wang YL, Dai XK, Xie CB. Dosimetric comparison between helical tomotherapy and intensity-modulated radiation therapy plans for non-small cell lung cancer. *Chin Med J*. 2011;124:1667–71.
- Song CH, Pyo H, Moon SH, Kim TH, Kim DW, Cho KH. Treatment-related pneumonitis and acute esophagitis in non-small-cell lung cancer patients treated with chemotherapy and helical tomotherapy. *Int J Radiat Oncol Biol Phys*. 2010;78:651–8.
- Liu HH, Jauregui M, Zhang X, Wang X, Dong L, Mohan R. Beam angle optimization and reduction for intensity-modulated radiation therapy of non-small-cell lung cancers. *Int J Radiat Oncol Biol Phys*. 2006;65:561–72.
- Lin CT, Shiau AC, Tien HJ, Yeh HP, Shueng PW, Hsieh CH. An attempted substitute study of total skin electron therapy technique by using helical photon tomotherapy with helical irradiation of the total skin treatment: a phantom result. *Biomed Res Int*. 2013;2013:108794.
- Reynders T, Tournel K, De Coninck P, Heymans S, Vinh-Hung V, Van Parijs H, et al. Dosimetric assessment of static and helical TomoTherapy in the clinical implementation of breast cancer treatments. *Radiat Oncol*. 2009;93:71–9.
- Otto K. Volumetric modulated arc therapy: IMRT in a single gantry arc. *Med Phys*. 2008;35:310–7.
- CX Y, Tang G. Intensity-modulated arc therapy: principles, technologies and clinical implementation. *Phys Med Biol*. 2011;56:R31–54.
- Murai T, Shibamoto Y, Manabe Y, Murata R, Sugie C, Hayashi A, et al. Intensity-modulated radiation therapy using static ports of tomotherapy (TomoDirect): comparison with the TomoHelical mode. *Radiat Oncol*. 2013;8:68.
- Chen M, Chen Y, Chen Q, Lu W. Theoretical analysis of the thread effect in helical TomoTherapy. *Med Phys*. 2011;38:5945–60.
- Sini C, Broggi S, Fiorino C, Cattaneo GM, Calandrino R. Accuracy of dose calculation algorithms for static and rotational IMRT of lung cancer: a phantom study. *Phys Med*. 2015;31:382–90.
- Zhao Y, Qi G, Yin G, Wang X, Wang P, Li J, et al. A clinical study of lung cancer dose calculation accuracy with Monte Carlo simulation. *Radiat Oncol*. 2014;9:287.
- Radiation Therapy Oncology Group (RTOG 0617): A randomized phase III comparison of standard dose (60Gy) versus high-dose (74Gy) conformal radiotherapy with concurrent and consolidation carboplatin/paclitaxel in patients with stage IIIA/IIIB non-small cell lung cancer. 2008. <http://www.rtog.org/ClinicalTrials/ProtocolTable/StudyDetails.aspx?action=openFile&FileID=4649>.
- van't Riet A, Mak AC, Moerland MA, Elders LH, van der Zee W. A conformation number to quantify the degree of conformality in brachytherapy and external beam irradiation: application to the prostate. *Int J Radiat Oncol Biol Phys*. 1997;37:731–6.

37. Hong CS, SG J, Kim M, Kim JI, Kim JM, Suh TS, et al. Dosimetric effects of multileaf collimator leaf width on intensity-modulated radiotherapy for head and neck cancer. *Med Phys*. 2014;41:021712.
38. Belderbos J, Heemsbergen W, Hoogeman M, Pengel K, Rossi M, Lebesque J. Acute esophageal toxicity in non-small cell lung cancer patients after high dose conformal radiotherapy. *Radiother Oncol*. 2005;75:157–64.
39. Emami B, Lyman J, Brown A, Coia L, Goitein M, Munzenrider JE, et al. Tolerance of normal tissue to therapeutic irradiation. *Int J Radiat Oncol Biol Phys*. 1991;21:109–22.
40. Gagliardi G, Lax I, Rutqvist LE. Partial irradiation of the heart. *Semin Radiat Oncol*. 2001;11:224–33.
41. Hayman JA, Martel MK, Ten Haken RK, Normolle DP, Todd RF 3rd, Littles JF, et al. Dose escalation in non-small-cell lung cancer using three-dimensional conformal radiation therapy: update of a phase I trial. *J Clin Oncol*. 2001;19:127–36.
42. Kutcher GJ, Burman C. Calculation of complication probability factors for non-uniform normal tissue irradiation: the effective volume method. *Int J Radiat Oncol Biol Phys*. 1989;16:1623–30.
43. Song C, Pyo H, Kim J, Lim YK, Kim WC, Kim HJ, et al. Superiority of conventional intensity-modulated radiotherapy over helical tomotherapy in locally advanced non-small cell lung cancer. A comparative plan analysis. *Strahlenther Onkol*. 2012;188:901–9.
44. Brink C, Berg M, Nielsen M. Sensitivity of NTCP parameter values against a change of dose calculation algorithm. *Med Phys*. 2007;34:3579–86.
45. Hedin E, Back A. Influence of different dose calculation algorithms on the estimate of NTCP for lung complications. *J Appl Clin Med Phys*. 2013;14:127–39.
46. Li H, Park P, Liu W, Matney J, Liao Z, Balter P, et al. Patient-specific quantification of respiratory motion-induced dose uncertainty for step-and-shoot IMRT of lung cancer. *Med Phys*. 2013;40:121712.
47. Duan J, Shen S, Fiveash JB, Popple RA, Brezovich IA. Dosimetric and radiobiological impact of dose fractionation on respiratory motion induced IMRT delivery errors: a volumetric dose measurement study. *Med Phys*. 2006;33:1380–7.
48. Jiang SB, Pope C, Al Jarrah KM, Kung JH, Bortfeld T, Chen GT. An experimental investigation on intra-fractional organ motion effects in lung IMRT treatments. *Phys Med Biol*. 2003;48:1773–84.
49. Chan OS, Lee MC, Hung AW, Chang AT, Yeung RM, Lee AW. The superiority of hybrid-volumetric arc therapy (VMAT) technique over double arcs VMAT and 3D-conformal technique in the treatment of locally advanced non-small cell lung cancer—a planning study. *Radiother Oncol*. 2011;101:298–302.
50. Jiang X, Li T, Liu Y, Zhou L, Xu Y, Zhou X, et al. Planning analysis for locally advanced lung cancer: dosimetric and efficiency comparisons between intensity-modulated radiotherapy (IMRT), single-arc/partial-arc volumetric modulated arc therapy (SA/PA-VMAT). *Radiat Oncol*. 2011;6:140.
51. Schallenkamp JM, Miller RC, Brinkmann DH, Foote T, Garces YI. Incidence of radiation pneumonitis after thoracic irradiation: dose-volume correlates. *Int J Radiat Oncol Biol Phys*. 2007;67:410–6.

Submit your next manuscript to BioMed Central and we will help you at every step:

- We accept pre-submission inquiries
- Our selector tool helps you to find the most relevant journal
- We provide round the clock customer support
- Convenient online submission
- Thorough peer review
- Inclusion in PubMed and all major indexing services
- Maximum visibility for your research

Submit your manuscript at  
[www.biomedcentral.com/submit](http://www.biomedcentral.com/submit)

